A Drop-on-Micropillars (DOM) based Acoustic Wave Viscometer for High Viscosity Liquid Measurement

Ilia chiniforooshan Esfahani, Hongwei Sun*

*Corresponding author: ho.sun@northeastern.edu

Mechanical and Industrial Engineering, Northeastern University, Boston, MA, 02215, USA

Abstract

High viscosity measurement is critical for many applications such as food manufacturing, drug development and biomedical diagnostics. Vibration-based viscosity measurement devices have become increasingly popular due to their portability, cost efficiency, ease of maintenance, and low sample consumption. However, they suffered some drawbacks such as low sensitivity and high damping and noise levels when measuring high viscosity liquids due to the increased hydrodynamic loading on the vibrating structures. In this work, a novel drop-on-micropillar (DOM) concept is developed to significantly improve the sensitivity and reduce the damping of the vibrational viscometers by making use of a liquid drop on a micropillar array under non-wetting state and in the meantime, generating a unique resonance phenomenon between micropillars and acoustic wave substrate - quartz crystal resonator (QCR). The DOM device was realized by fabricating polymethyl methacrylate (PMMA) square micropillars on a QCR surface by thermal nanoimprinting lithography (T-NIL), and the micropillar surface was then modified through chemical vapor deposition (CVD) technique to yield a superhydrophobic surface. The resonance frequency shifts and quality factors of the devices were measured for deionized (DI) water and aqueous glycerol solution with viscosity ranging from 3 cP to 91.4 cP. The results show that the DOM devices can achieve the measurement of viscous liquids at a high sensitivity while maintaining the quality factor (energy dissipation) within very low levels. Furthermore, a theoretical model was successfully developed to predict the frequency shift and quality factor of the DOM devices by integrating the Euler-Bernoulli beam theory with the small load approximation of QCR.

Keywords: acoustic wave, micropillars, viscosity measurement, wetting states

1. Introduction

Measuring the viscosity of fluids is essential in various applications such as food manufacturing [1], drug development [2], and biomedical diagnostics [3]. Conventional benchtop viscosity measurement equipment including falling-body, capillary, rotational, and vibrational viscometers are large, expensive, and require large sample volumes for viscosity measurement [4]. With the advancement of micro- and nanofabrication technologies, vibration-based viscosity measurements devices such as microcantilever and quartz crystal resonator (QCR) have become increasingly popular due to their portability, cost efficiency, ease of maintenance, and low sample consumption [5, 6]. For instance, piezoelectrically driven cantilever beam viscometers have been successfully used to track the viscosity of a sample fluid based on the resonance frequency shift caused by fluid-structure interaction (FSI) [7]. To enhance the sensitivity of frequency-based viscometers, crystal resonators such as ZnO, quartz, and lithium niobate that operate in thickness shear mode (TSM) have been proposed [8]. Among different crystal resonators, the AT-cut quartz crystal microbalance (QCM) has become very attractive due to its low-cost fabrication, availability, and insensitivity to temperature [9, 10]. The frequency shift of the QCM viscometer in response to the liquid viscosity changes is described by the Kanazawa theory, described as [11]:

$$\Delta f = -\frac{f_0^{3/2}}{Z_q}\sqrt{\frac{\rho_L \eta_L}{\pi}} \tag{1}$$

Where f_0 is fundamental quartz resonance frequency, Z_q is quartz acoustic impedance, ρ_L is the medium density and η_L is the medium viscosity. For example, Ash et al. employed QCM to characterize the viscosity of various industrial oils by only a droplet of sample solution [12]. The device demonstrated the capability of distinguishing oils with viscosities less than 500 cP. The QCM was also used to measure aqueous rabbit blood viscosity with the assistance of powerful oscillating circuits and impedance analysis methods [13]. It shows that the QCM with impedance analysis method was capable of measuring the blood viscosity with an accuracy of 1.8% for a blood volume of 17.5 μL.

Despite the great potential in measuring liquid viscosity, vibration-based viscometers face several drawbacks, such as low sensitivity and high damping and noise levels when measuring high viscosity liquids in comparison to conventional rotational and pressure-sensing viscometers [14]. Recently, a novel acoustic wave based sensing mechanism was discovered by imprinting polymer micropillars on the acoustic wave substrate (μPAW), leading to a two-degree-of-freedom vibration system [15]. Because of the resonance of micropillars and acoustic wave substrate, the μPAW devices demonstrated a maximum mass sensitivity of 27-fold compared to conventional QCM in detecting bovine serum albumin (BSA) adhesion on the substrate [16]. The μPAW technology has also shown a higher sensitivity in measuring viscosity but suffers from significant energy dissipation or damping, especially for viscous liquids such as blood [17].

To overcome the high energy dissipation and further broaden the range of viscosity measurement of the μPAW technology, a novel concept based on suspending a sample drop on a micropillar array (DOM) is developed in this research. As we know, the droplet can form two stable wetting states on a micropillar surface – Cassie state and Wenzel state [18, 19]. In the Cassie state, the drop sits on the tops of the micropillars and the air fills in between the micropillars, while in the Wenzel state, the cavities between micropillars are filled by the liquid, resulting in an entire immersion of micropillars in the liquid. In the DOM concept, the micropillars surfaces were modified to be hydrophobic to produce the Cassie wetting state for the liquid. As a result, only the tops of the micropillars are in contact with the liquid for the viscosity measurement purpose. In this way, the DOM device can maintain the high sensitivity of the μPAW technology dye to the resonance of micropillars and acoustic wave substrate while avoiding the high energy dissipation (damping) caused by the surrounding liquid loading to the micropillars. As a demonstration, Figure 1 shows the impedance spectrum and Q-factors [20] of a μPAW device when a DI water drop was pipette-dropped on a micropillar array (side length:10 μm, spacing: 21 μm and pillar height: 13.9 μm) under Cassie and Wenzel wetting states. It clearly shows that the Q-factor increases from 46 to 654 when the wetting state changes from Wenzel state to Cassie state which means significant improvement in damping and noise in the frequency measurement.

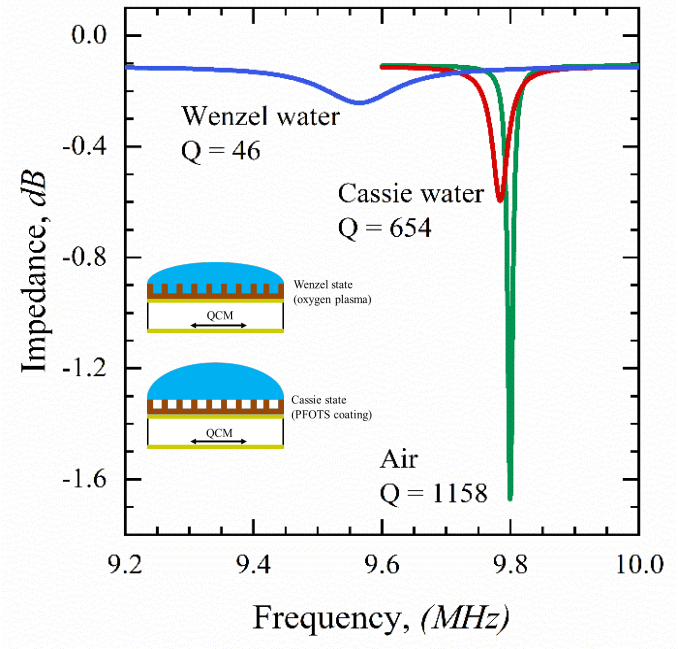

Figure 1. Impedance spectrum and Q-factors of a water drop on square-shaped micropillars (side length:10 μm, spacing: 21 μm and height:13.9 μm) on a QCR substrate under Cassie and Wenzel states

In this study, polymethyl methacrylate (PMMA) square micropillars were fabricated on a quartz crystal plate surface by thermal nanoimprinting lithography (T-NIL). The surface of PMMA micropillars were then modified through chemical vapor deposition (CVD) to produce a superhydrophobic wetting state. Glycerol solutions with viscosities ranging from 3 cP (30 % V/V) to 91.4 cP (80 % V/V) were measured using the proposed DOM device. Furthermore, a theoretical study was performed based on the Euler-Bernoulli beam theory to understand the behavior of the drop-on-micropillar (DOM) viscometer and predict the Q-factor of the devices.

2. Experimental Method

2.1. Preparation of DOM device

AT-cut quartz crystal resonators of the resonance frequency of 10 MHz (thickness: 167μm) (Fortiming, MA) with coated 100 nm-thickness gold films on top and bottom surfaces were

purchased as the substrate of DOM devices. The PMMA powder was purchased from Kayaku Advanced Materials (Westborough, MA), and the PMMA micropillars were directly fabricated on the QCR substrate using T-NIL (NX-2600, Nanonex, NJ). The detailed fabrication procedure was reported elsewhere [15]. The nanoimprinted PMMA micropillars have a square-shaped cross-section with a side length of 10 μm. The center-to-center spacing of micropillars are 21 μm, and the heights are 6.4 μm, 10.3 μm, 11.5 μm, 13.9 μm, and 18.1 μm, respectively. To create Cassie state, the surface of PMMA micropillars was coated with a 1H,1H,2H,2H-perfluoroctyltriethoxysilane (PFOTS, C14H19F13O3Si, Sigma-Aldrich, MO) film using chemical vapor deposition (CVD) method. During the coating process, the micropillar film was placed in a vacuum drying chamber at 80 mTorr with a drop of PFOTS for 24 hours at room temperature to ensure all pillar surfaces were uniformly coated with PFOTS molecules. For the purpose of comparison, another micropillar film was treated in an oxygen plasma chamber (PDC32 G, Harrick Plasma, NY) at a power of 18 W for 30 seconds. It shows that the hydroxyl groups (O-H bonds) generated by the oxygen plasma treatment resulted in a superhydrophilic surface.

2.2. Experimental system

Figure 2 shows the experimental setup for the viscosity measurement using the DOM device consisting of a micropillar enhanced acoustic wave device, a network analyzer (HP8753D, Agilent Technologies, CA), and a PC with in-house data acquisition system (LABVIEW, National Instruments). The admittance spectrum of the frequency signal from the DOM device was measured by the network analyzer and transmitted to the PC via a GPIB board. The resonance frequency, bandwidth, and Q-factor of the signal were extracted by fitting the spectrum into a Lorentzian curve with the in-house LabView program. During the experiment, a liquid drop of 150 μL was gently loaded on the micropillar surface by a pipette (USA Scientific, FL) to completely cover the sensing area. During the measurement, a control experiment was conducted using DI water to establish a baseline first. Then measurements were conducted for aqueous glycerol solutions (Sigma-Aldrich., MO) with concentrations ranging from 30% (3 cP) to 80 % V/V (91.4 cP). All the experiments were repeated three times to ensure the reproducibility of the measurements.

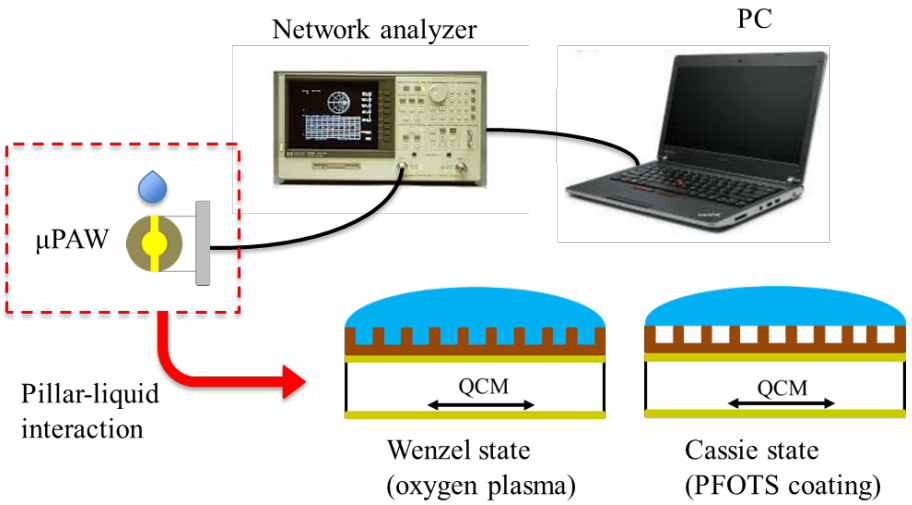

Figure 2. Schematic of experimental setup for viscosity measurement

3. Theoretical Model

3.1. Equivalent circuit model

The Butterworth-van-Dyke (BVD) equivalent electrical circuit [21, 22] was modified to study the DOM device operating in a liquid medium, as shown in Figure 3.

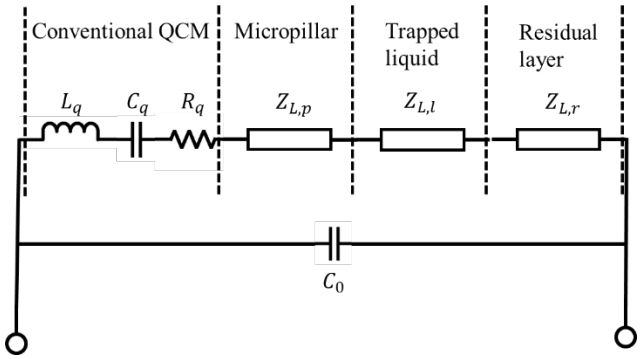

Figure 3. Modified Butterworth-van Dyke (BVD) equivalent circuit for μPAW operating in a liquid medium

It should be noted that the quartz crystal plate between the two gold electrodes of the QCR is represented as a parallel capacitance (C_0) in the electrical branch. The inertia, compliance, and damping properties of a QCR are represented by an inductance (L_1), a capacitance (C_1), and a resistance (R_1) in the acoustic branch, respectively. $Z_{L,p}$ is the load impedance induced by the

micropillars and pillar-liquid interaction. The trapped liquid between micropillars acts as an additional loading on the QCM ($Z_{L,l}$) which is described by Kanazawa theory as [11]:

$$Z_{L,l} = \frac{\eta_l (1+i)}{\delta} \tag{2}$$

where δ is the thickness of the layer of the liquid surrounding the cantilever, which is defined by:

$$\delta = \sqrt{\frac{2\eta_L}{\omega \rho_L}} \tag{3}$$

A thin PMMA residual layer (h_r = 3 μm) was produced during T-NIL process, and the load impedance of the layer ($Z_{L,r}$) is represented as:

$$Z_{L,r} = \omega \rho_P h_r i \tag{4}$$

The total load impedance induced by the micropillars on the QCR (Z_{tot}) can be calculated as:

$$Z_{L,tot} = Z_{L,p} + Z_{L,l} + Z_{L,r} \tag{5}$$

Based on small load approximation (SLA), the resonance frequency (f), half-bandwidth (HBW) (Γ), and Q-factor (Q) of the QCR device due to the additional load can be expressed as [23-25]:

$$f = f_0 - \frac{f_0}{\pi} Re\left(\frac{iZ_{L,tot}}{Z_q}\right) \tag{6a}$$

$$\Gamma = \Gamma_0 + \frac{f_0}{\pi} imag\left(\frac{iZ_{L,tot}}{Z_q}\right) \tag{6b}$$

$$Q = \frac{f}{2\Gamma} \tag{6c}$$

Where f_o and Γ_0 are the fundamental resonance frequency and HBW of quartz resonator in air. The load impedance $Z_{L,p}$ induced by micropillar vibration in the liquid under Cassie and Wenzel states are described below.

3.2. Load impedance induced by micropillars in Wenzel state

The micropillar can be treated as a uniform Euler-Bernoulli beam oscillating in a liquid. The governing equation is given by [26]:

$$\frac{d^4\widehat{W}(\hat{x}|\omega)}{d\hat{x}^4} - \frac{\dot{m}\omega^2 L^4}{EI}\left(1 + \frac{\pi\rho_p b^2}{4\dot{m}}\gamma(\omega)\right)\widehat{W}(\hat{x}|\omega) = 0 \tag{7}$$

The associated boundary conditions are given below:

$$\widehat{W}(0|\omega) = u_0 \tag{8a}$$

$$\frac{d\widehat{W}(0|\omega)}{d\hat{x}} = 0 \tag{8b}$$

$$\frac{d^2\widehat{W}(1|\omega)}{d\hat{x}^2} = 0 \tag{8c}$$

$$\frac{d^3\widehat{W}(1|\omega)}{d\hat{x}^3} = 0 \tag{8d}$$

Where ω is the angular frequency of the micropillar, E is the young modulus of micropillars, and I the momentum of inertia of micropillars. $\dot{m}$ is the mass per unit length of the micropillar and ρ_p is the density of micropillars. u_0 is the displacement of the top surface of the quartz plate. The solution of Eq. 7 takes the form of (see Supplementary Material for details):

$$\widehat{W}(\hat{x}|\omega) = u_0(C_1\cos(\beta\hat{x}) + C_2\sin(\beta\hat{x}) + C_3\cosh(\beta\hat{x}) + C_4\sinh(\beta\hat{x})) \tag{9}$$

Where

$$\beta^4 = \frac{\dot{m}\omega^2 L^4}{EI}\left(1 + \frac{\pi\rho_p b^2}{4\dot{m}}\gamma(\omega)\right) \tag{10}$$

As a result, the load impedance ($Z_{L,p}$) caused by micropillars can be calculated as:

$$Z_{L,p} = \frac{\tau}{v_0} = \frac{EI\beta^3(C_4 - C_2)}{AL^3\omega i} \tag{11}$$

Where A is the area of a unit cell of micropillar, τ is the tangential stress, and v_0 is the tangential velocity. Therefore, the total load impedance (Z_{tot}) can be written as

$$Z_{tot} = \frac{EI\beta^3(C_4 - C_2)}{AL^3\omega i} + \frac{\eta_l\,(1+i)}{\delta} + \omega\rho_P h_r i \tag{12}$$

3.3. Load impedance induced by micropillars in Cassie state

When the μPAW device operates in the Cassie state (DOM), only the tops of the micropillars interact with the liquid. The governing equation for the vibration of a uniform Euler-Bernoulli beam reduces to:

$$\frac{d^4\widehat{W}(\hat{x}|\omega)}{d\hat{x}^4} - \frac{\dot{m}\omega^2 L^4}{EI}\widehat{W}(\hat{x}|\omega) = 0 \tag{14}$$

The oscillating liquid layer on the tops is treated as a damper to the micropillars, and the complex wall shear stress acting on the top can be determined as [11, 27]:

$$F_t = \frac{b^2\eta_L\omega}{\delta}\widehat{W}(L|\omega)(1+i) \tag{13}$$

With its associated boundary conditions as:

$$\widehat{W}(0|\omega) = u_0 \tag{15a}$$

$$\frac{d\widehat{W}(0|\omega)}{d\hat{x}} = 0 \tag{15b}$$

$$\frac{d^2\widehat{W}(1|\omega)}{d\hat{x}^2} = 0 \tag{15c}$$

$$EI\frac{d^3\widehat{W}(1|\omega)}{d\hat{x}^3} + F_t = 0 \qquad (15d)$$

The nontrivial solution has a similar form as the previous one given by:

$$\widehat{W}(\hat{x}|\omega) = u_0(C_1\cos(\beta\hat{x}) + C_2\sin(\beta\hat{x}) + C_3\cosh(\beta\hat{x}) + C_4\sinh(\beta\hat{x})) \qquad (16)$$

Where:

$$\beta^4 = \frac{\dot{m}\omega^2 L^4}{EI} \qquad (17)$$

As a result, the total load impedance on the QCM substrate for DOM becomes:

$$Z_{tot} = \frac{EI\beta^3(C_4 - C_2)}{AL^3\omega i} + \omega\rho_P h_r i \qquad (24)$$

It should be noted that the load impedance due to the trapped liquid ($Z_{L,l}$) is not included.

4. Results and Discussion

4.1. DI water measurement

For the purpose of comparison, the DOM based μPAW device was operating in air and DI water under Cassie (suspended) and Wenzel (fully penetrated) states. The results are presented in Fig. 4.

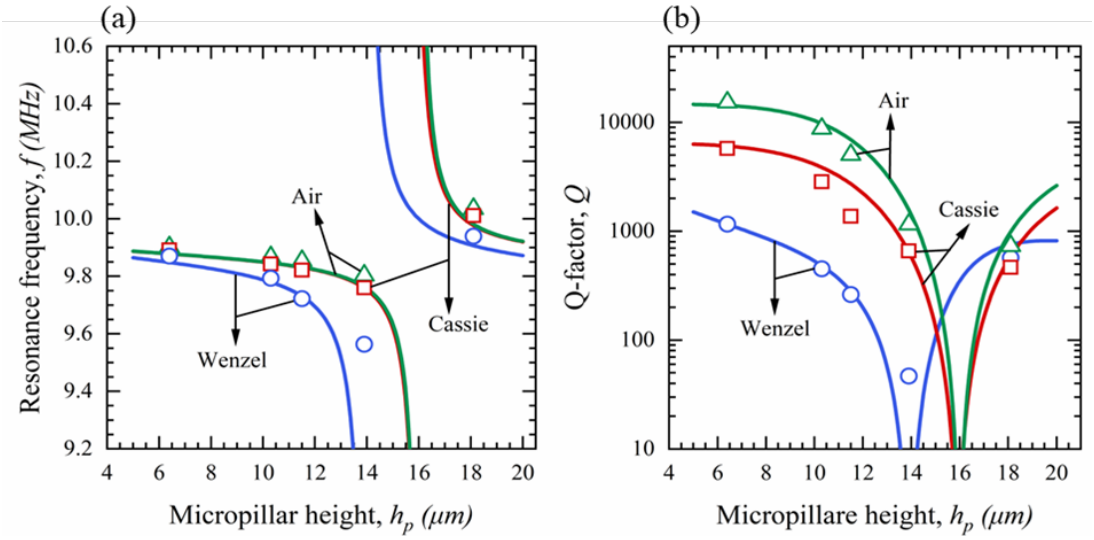

Figure 4. Comparison of model predictions of (a) resonance frequency (f) and (b) Q-factor (Q) operating in air, Cassie, and Wenzel states with measured values

It can be seen that a coupled resonance phenomenon took place between the quartz crystal plate and the micropillars yielding a nonlinear resonance frequency and corresponding Q-factor response vs. micropillar heights. As micropillar height or the mass of micropillars increases, the

resonance frequency decreases, which is consistent with Sauerbrey theory [28]. When the micropillar height approaches a critical height, a sudden drop and jump behavior is observed due to the coupling between the micropillars and the quartz crystal resonator. In the meantime, the Q-factor of μPAW decreases as well with the increase of micropillar height. It is believed that two factors contribute to the reduction in Q-factor: 1) increasing the thickness of PMMA film will result in increased acoustic energy dissipation in the polymer; 2) when the height of the micropillar approaches the "critical height," the oscillating micropillars act as a dynamic vibration absorber, absorbing the majority of the acoustic energy from the QCM which in turn reduces the Q-factor until it reaches its minimum value at a critical height.

The modeling results shown in Figure 4 (a) demonstrate the capability of the model in predicting the resonance frequency and Q-factor of the devices acting in DI water under the Cassie and Wenzel states. It is worth noting that the μPAW device with the superhydrophilic surface (fully penetrated state) shows more frequency shifts in comparison to the DOM devices with superhydrophobic surfaces (Cassie state). This is mainly due to more liquid between micropillars was moving with micropillars when the device is in the Wenzel state, while for the DOM device, only the liquid on the micropillar tops was disturbed by the vibration of the micropillars. Furthermore, the critical height of the DOM device (~15.8 μm) is very close to that of the μPAW in the air (~16 μm). However, liquid penetration in the Wenzel state results in a shift in the critical height (~14 μm) due to the induced hydrodynamic loadings on the micropillars. Figure 4(b) also shows μPAW operating in DI water displays a much lower Q-factor than in the air due to the liquid damping. A 50% reduction in Q-factor was observed for the DOM device in water compared to the air. However, the Q-factor is reduced by orders of magnitude in the Wenzel state due to the complete penetration of the liquid. It can be noticed that the minimum Q-factor occurred when the micropillar height approached its respective critical heights independent of the wetting conditions.

4.2. Effect of wetting states

Figure 5(a) presents the effect of the wetting state on the resonance frequency shift of μPAW operating in glycerol solution with a concentration of 40 V/V% (viscosity: 4.8 cP). The experimental results show that the μPAW devices in the Wenzel state show higher frequency shifts than DOM based μPAW devices in the Cassie state due to the existence of liquid between micropillars. The reason is that for the devices operating in the Cassie state, liquid-micropillar

interactions occur only at the tops of the micropillars. The DOM based μPAW device in the Cassie state shows a maximum frequency shift of 14.8 kHz, while the shift in the Wenzel state increases to a maximum value of 41.3 kHz as the micropillar height approaches the Wenzel state critical height. Figure 6(b) illustrates the Q-factor measurement for both devices in different wetting states. As can be seen, the Q-factors of μPAW depends on both the height and hydrophobicity of the micropillars. The Q-factor of superhydrophilic micropillars is typically one order of magnitude lower than superhydrophobic micropillars, resulting in a significantly higher noise level.

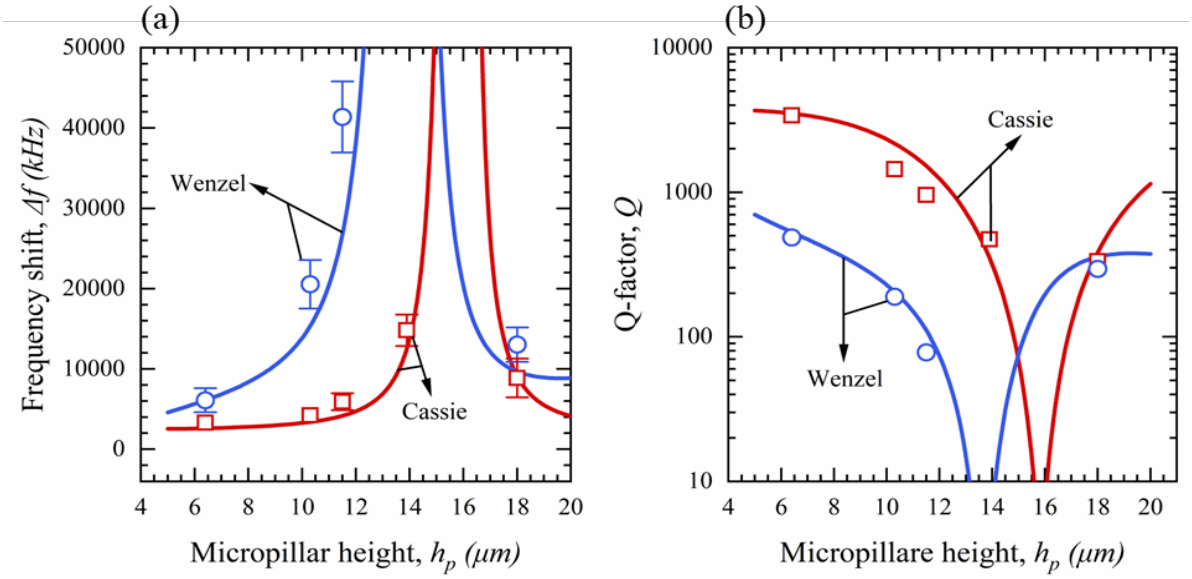

Figure 5. Model prediction for frequency shift (a) and Q-factor (b) of μPAW in glycerol solution (c = 40 V/V%) vs. measured values

4.3.Glycerol solution measurement

To demonstrate the capability for the viscosity measurement, a DOM based μPAW device with a micropillar height of 11.5 μm was used for glycerol solutions with viscosity ranging from 3 cP to 91.4 cP (concentration: 30 to 80 % V/V) under Cassie and Wenzel states. The results of the frequency shift and Q-factor are shown in Figure 6. It can be seen that as the viscosity of the solution increases, the frequency shift increases, and the Q-factor decreases due to increasing penetration layer thickness and energy dissipation of the micropillars. The μPAW device operating in the Wenzel state can only measure the viscosity up to 16 cP (60 % V/V) due to a significantly low Q-factor (below 50). However, the DOM based μPAW device can significantly improve the

Q-factor level and extend the viscosity range over 90 cP while maintaining the Q-factor within an acceptable level (>100).

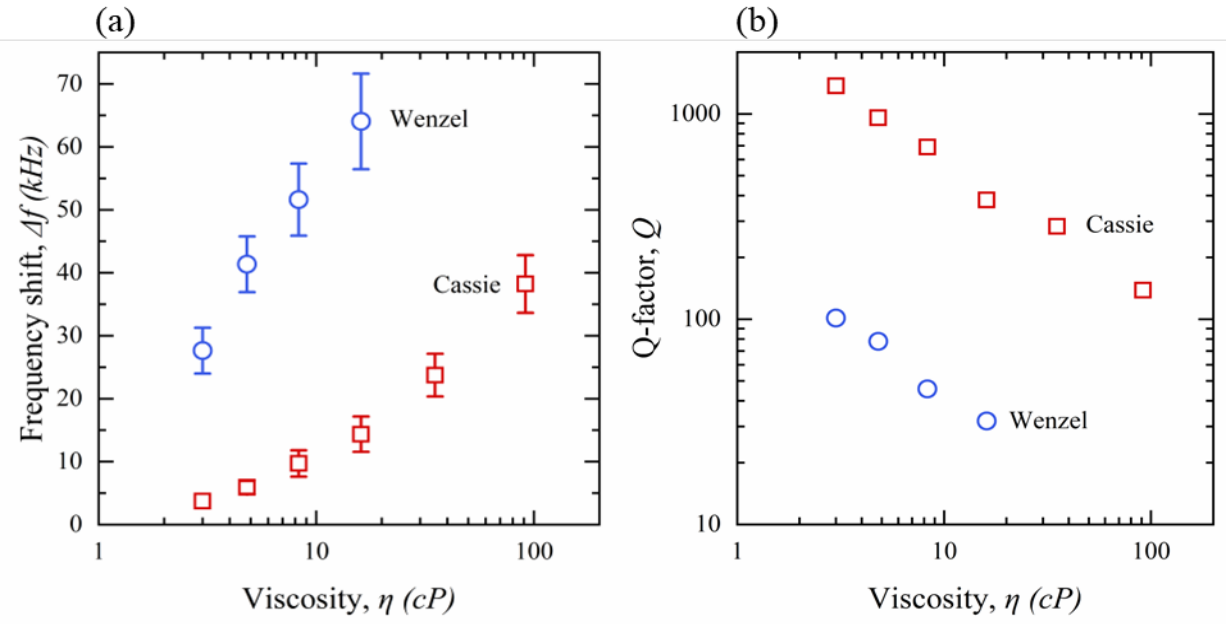

Figure 6. Viscosity measurement results of (a) frequency shift and (b) Q-factor of μPAW operating in Cassie and Wenzel states for glycerol solutions ranging from 3 cP to 91.4 cP

5. Conclusions

The performance of the drop-on-micropillar (DOM) concept based micropillar-enhanced acoustic wave devices was investigated experimentally and theoretically for viscosity measurement of aqueous glycerol solutions with viscosity ranging from 3 cP to 91.4 cP. The results demonstrated that superhydrophobic micropillars can provide a reliable Cassie wetting state which is critical for measuring high viscosity liquid at a high sensitivity and enhanced Q-factor in comparison to hydrophilic micropillars. The micropillars vibrating under Cassie state have a much-reduced energy dissipation caused by weak interactions between pillars and air trapped between micropillars. On the other hand, the micropillar-enhanced acoustic wave device operating in a fully penetrated wetting state suffers high energy dissipation due to the increased damping effect from the liquid and rapidly decreased Q-factor. The theoretical model based on the Euler-Bernoulli beam theory and the small load approximation can accurately predict the frequency shift and quality factor of the DOM devices. It is evident that employing the DOM concept provides a new way of measuring high-viscosity solutions using micropillar-enhanced acoustic wave devices.

Declaration of Competing Interest

The authors declare that they have no known competing financial interests or personal relationships that could have appeared to influence the work reported in this paper.

Data availability

Data will be made available on request.

Acknowledgment

The authors thank MicroChem Corp. (Westborough, MA, USA) for providing PMMA material and financial support from National Science Foundation (NSF ECCS 2130716).

References

[1] G. Tucker, Applications of rheological data in the food industry, Advances in Food Rheology and Its Applications, Elsevier2023, pp. 181-200.

[2] X. Yang, D. Zhang, Y. Ye, Y. Zhao, Recent advances in multifunctional fluorescent probes for viscosity and analytes, Coordination Chemistry Reviews, 453(2022) 214336.

[3] H. Kang, I. Jang, S. Song, S.-C. Bae, Development of a paper-based viscometer for blood plasma using colorimetric analysis, Analytical chemistry, 91(2019) 4868-75.

[4] S. Puneeth, M.B. Kulkarni, S. Goel, Microfluidic viscometers for biochemical and biomedical applications: A review, Engineering Research Express, 3(2021) 022003.

[5] P. Singh, P.B. Agarwal, A comprehensive review on MEMS-based viscometers, Sensors and Actuators A: Physical, (2022) 113456.

[6] N. Farsaei Vahid, M.R. Marvi, M.R. Naimi-Jamal, S.M. Naghib, A. Ghaffarinejad, Effect of surfactant type on buckypaper electrochemical performance, Micro & Nano Letters, 13(2018) 927-30.

[7] H. Elahi, M. Eugeni, P. Gaudenzi, A review on mechanisms for piezoelectric-based energy harvesters, Energies, 11(2018) 1850.

[8] Y. Huang, P.K. Das, V.R. Bhethanabotla, Surface acoustic waves in biosensing applications, Sensors and Actuators Reports, 3(2021) 100041.

[9] J. Hu, X. Huang, QCM mass sensitivity analysis based on finite element method, IEEE Transactions on Applied Superconductivity, 29(2018) 1-4.
[10] S. Ji, R. Ran, I. Chiniforooshan Esfahani, K.-t. Wan, H. Sun, A New Microfluidic Device Integrated With Quartz Crystal Microbalance to Measure Colloidal Particle Adhesion, ASME International Mechanical Engineering Congress and Exposition, American Society of Mechanical Engineers2021, p. V005T05A75.
[11] K.K. Kanazawa, J.G. Gordon, Frequency of a quartz microbalance in contact with liquid, Analytical Chemistry, 57(1985) 1770-1.
[12] D.C. Ash, M.J. Joyce, C. Barnes, C.J. Booth, A.C. Jefferies, Viscosity measurement of industrial oils using the droplet quartz crystal microbalance, Measurement Science and Technology, 14(2003) 1955.
[13] S. Liao, P. Ye, C. Chen, J. Zhang, L. Xu, F. Tan, Comparing of Frequency Shift and Impedance Analysis Method Based on QCM Sensor for Measuring the Blood Viscosity, Sensors, 22(2022) 3804.
[14] L. Rodriguez-Pardo, J.F. Rodríguez, C. Gabrielli, H. Perrot, R. Brendel, Sensitivity, noise, and resolution in QCM sensors in liquid media, IEEE Sensors Journal, 5(2005) 1251-7.
[15] P. Wang, J. Su, W. Dai, G. Cernigliaro, H. Sun, Ultrasensitive quartz crystal microbalance enabled by micropillar structure, Applied Physics Letters, 104(2014) 043504.
[16] J. Su, H. Esmaeilzadeh, F. Zhang, Q. Yu, G. Cernigliaro, J. Xu, et al., An ultrasensitive micropillar-based quartz crystal microbalance device for real-time measurement of protein immobilization and protein-protein interaction, Biosensors and Bioelectronics, 99(2018) 325-31.
[17] I.C. Esfahani, H. Sun, A droplet-based micropillar-enhanced acoustic wave (μPAW) device for viscosity measurement, Sensors and Actuators A: Physical, (2022) 114121.
[18] A. Cassie, Contact angles, Discussions of the Faraday society, 3(1948) 11-6.
[19] R.N. Wenzel, Surface roughness and contact angle, The Journal of Physical Chemistry, 53(1949) 1466-7.
[20] M. Rodahl, F. Höök, A. Krozer, P. Brzezinski, B. Kasemo, Quartz crystal microbalance setup for frequency and Q-factor measurements in gaseous and liquid environments, Review of Scientific Instruments, 66(1995) 3924-30.
[21] S. Butterworth, On electrically-maintained vibrations, Proceedings of the Physical Society of London (1874-1925), 27(1914) 410.

[22] K.S. Van Dyke, The piezo-electric resonator and its equivalent network, Proceedings of the Institute of Radio Engineers, 16(1928) 742-64.
[23] D. Johannsmann, Viscoelastic, mechanical, and dielectric measurements on complex samples with the quartz crystal microbalance, Physical Chemistry Chemical Physics, 10(2008) 4516-34.
[24] W. Mason, Viscosity and shear elasticity measurements of liquids by means of shear vibrating crystals, Journal of colloid science, 3(1948) 147-62.
[25] H. Schilling, W. Pechhold, Two Quartz Resonator Methods for the Investigation of the Complex Shear Modulus of Polymers, Acta Acustica united with Acustica, 22(1969) 244-53.
[26] J.E. Sader, Frequency response of cantilever beams immersed in viscous fluids with applications to the atomic force microscope, Journal of applied physics, 84(1998) 64-76.
[27] H. Esmaeilzadeh, K. Zheng, C. Barry, J. Mead, M. Charmchi, H. Sun, Evaluating Superhydrophobic Surfaces under External Pressures using Quartz Crystal Microbalance, Langmuir, 37(2021) 6650-9.
[28] G. Sauerbrey, Verwendung von Schwingquarzen zur Wägung dünner Schichten und zur Mikrowägung, Zeitschrift für physik, 155(1959) 206-22.

Table of Contents Graphic

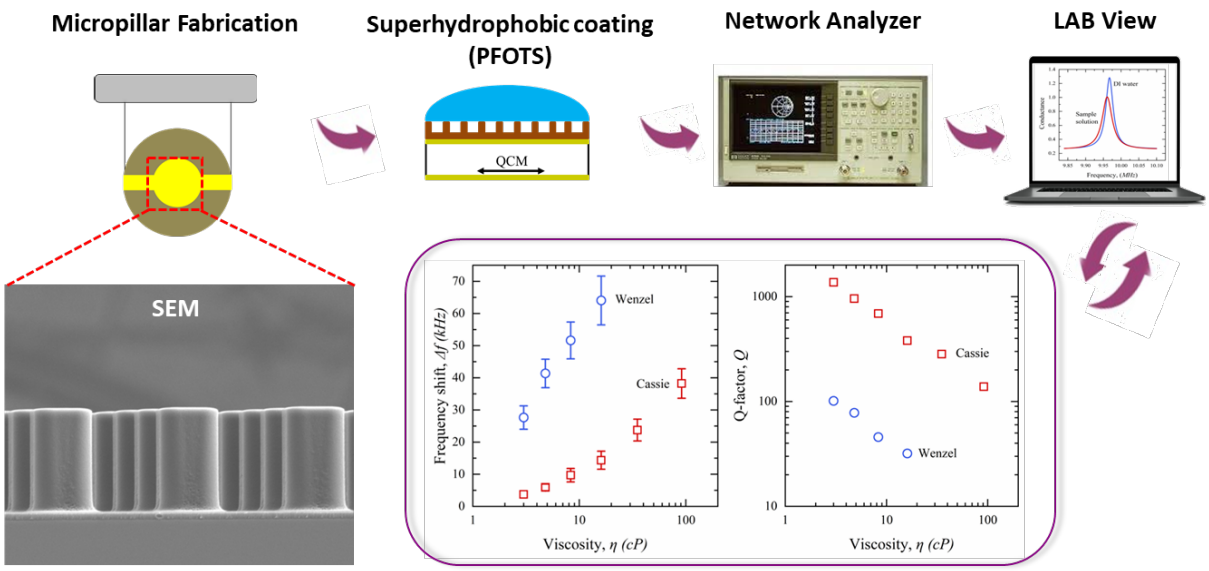
Micropillar Fabrication
Superhydrophobic coating (PFOTS)
Network Analyzer
LAB View
SEM
QCM
Wenzel
Cassie
Frequency shift, Δf (kHz)
Viscosity, η (cP)
Q-factor, Q
Viscosity, η (cP)